

# Collective Swimming and the Dynamics of Bacterial Turbulence

Charles W. Wolgemuth

University of Connecticut Health Center, Department of Cell Biology and Center for Cell Analysis and Modeling, Farmington, Connecticut 06030-3505

**ABSTRACT** To swim, a bacterium pushes against the fluid within which it is immersed, generating fluid flow that dies off on a length scale comparable to the size of the bacterium. However, in dense colonies of bacteria, the bacteria are close enough that flow generated by swimming is substantial. For these cases, complex flows can arise due to the interaction and feedback between the bacteria and the fluid. Recent experiments on dense populations of swimming *Bacillus subtilis* have revealed a volume fraction-dependent transition from random swimming to transient jet and vortex patterns in the bacteria/fluid mixture. The fluid motions that are observed are reminiscent of flows that are observed around translating objects at moderate to high Reynolds numbers. In this work, I present a two-phase model for the bacterial/fluid mixture. The model explains turbulent flows in terms of the dipole stress that the bacteria exert on the fluid, entropic elasticity due to the rod shape of each bacterium, and the torque on the bacteria due to fluid gradients. Solving the equations in two dimensions using realistic parameters, the model reproduces empirically observed velocity fields. Dimensional analysis provides scaling relations for the dependence of the characteristic scales on the model parameters.

## INTRODUCTION

The general dogma of fluid dynamics defines two distinct dynamical regimes that can be distinguished by the dimensionless Reynolds number ( $Re$ ), a ratio of inertia to viscosity. In terms of characteristic length and velocity scales,  $L$  and  $U$ , respectively,  $Re = UL/\eta$ , where  $\eta$  is the kinematic viscosity of the fluid. When  $Re < 1$ , which occurs at low velocities and small length scales, gradients in the hydrostatic pressure are balanced by viscous shear, the flow is smooth and laminar, and vortices are seldom seen. At large velocities and large length scales ( $Re \gg 1$ ), the viscosity is negligible compared to inertia. Therefore, gradients in the pressure act to accelerate the fluid. In this regime, sharp transitions in velocity are possible, which can be accompanied by vortices.

Bacterial swimming occurs in the low Reynolds number regime. For example, *Bacillus subtilis* is a rod-shaped cell that is roughly  $4\ \mu\text{m}$  long and  $0.7\ \mu\text{m}$  in diameter (1). At low concentrations, these cells swim at  $\sim 20\ \mu\text{m/s}$  (2). The Reynolds number for a single cell is therefore  $\sim 10^{-4}$ . As the cell concentration increases, fluid flow between neighboring cells will feel drag due to the velocity difference between the cells and the fluid. Therefore, one expects that as the bacterial concentration increases, the effective Reynolds number for the system should decrease. However, experiments on the swimming behavior and fluid dynamics in regions of high concentrations (in excess of  $10^9$  cells per  $\text{cm}^3$ ) of *B. subtilis* reveal very unexpected results (1,3). In these dense regions of bacteria, transient jet-like fluid motion occurs in which the speed of the jets is larger than the speed of an individual

bacterium ( $\sim 50\ \mu\text{m/s}$ ) (1). Furthermore, these jet-like regions are flanked by vortices that persist for timescales of  $\sim 1\ \text{s}$  (1). The fluid dynamics on length scales of  $100\text{--}200\ \mu\text{m}$  is reminiscent of a von Karman vortex street, which arises in fluids when the Reynolds number is  $> 50$  (4). Due to the qualitative similarity to high Reynolds number fluid dynamics, these swimming patterns have been termed bacterial “turbulence”.

This fluid behavior seems counterintuitive. If the bacteria move independently of the fluid, then the fluid flow must interpenetrate the dense suspension of bacteria. Increasing the concentration of the bacteria should increase the drag between fluid and the bacteria, thereby increasing the effective viscosity of the solution and lowering the Reynolds number. Yet, at face value, the opposite effect is seen; increasing the concentration of bacteria leads to fluid flows that seem to have a much higher Reynolds number. This leads to a number of interesting physical questions. What physics is required to describe the dynamical behavior of these systems? Can an effective Reynolds number for this system be defined, and, if so, how? What sets the length and timescales for the jets and vortices? Why are the velocities that are observed larger than the swimming velocity of an individual bacterium?

Recent theoretical work sheds some light on these issues. In Simha and Ramaswamy (5), the fluid stress from a collection of force dipoles was added to the Navier-Stokes equations. Linear analysis of this model in the low Reynolds number regime showed that it was unstable under large wavelength disturbances and that fluctuation in the number density of particles is anomalously large. Other authors have also used nematic hydrodynamic equations coupled to local stress generation to derive continuum equations for active filament solutions (6,7). These articles have shown that contractile activity can cause dramatic differences in rheological behavior and can lead to modulated flowing phases and macroscopic phase separation. Simulations of discrete numbers of

Submitted July 25, 2007, and accepted for publication March 3, 2008.

Address reprint requests to Charles W. Wolgemuth, Dept. of Cell Biology, University of Connecticut Health Center, 263 Farmington Ave., Farmington, CT 06030-3505. Tel.: (860) 679-1655; E-mail: [cwolgemuth@uchc.edu](mailto:cwolgemuth@uchc.edu).

Editor: Herbert Levine.

© 2008 by the Biophysical Society  
0006-3495/08/08/1564/11 \$2.00

doi: 10.1529/biophysj.107.118257

force dipoles (8) and extended dipole rods (9) have shown that vortices and jets can arise in these systems; however, these simulations neglected stochastic effects such as diffusion and run-and-tumble swimming of the bacteria.

In this work, I develop a two-phase model for the collective swimming of dense colonies of bacteria. This model treats the fluid and bacteria as independent, interpenetrating continuum phases. The bacteria are rod-like and therefore entropic effects will favor local alignment of the bacteria. Since the thrust on the bacteria comes from the flagellar bundle yet the drag on the bacteria acts on both the flagella and the cell body, the location of thrust is displaced from the center of drag, and the bacteria exert a dipole force on the fluid. Analysis of the run-and-tumble nature of bacterial swimming leads to a term that governs how tumbling can reorient the bacterial alignment. In this model, stochastic effects are treated using a mean-field approximation. For reasonable values of the model parameters, this model accurately reproduces the complex behavior observed in these systems and leads to a qualitative understanding of the length, time, and velocity scales that are present in the experiments.

## A two-phase model for collective bacterial swimming

The length scales over which vortical patterns and jets are observed in dense communities of swimming bacteria are much larger than the size of an individual bacterium. Therefore, on the scale of these flow patterns, it is reasonable to assume that the bacteria and the fluid can each be described as a continuum field. In this section, I develop a two-phase model to describe the average behavior of this system on these length scales. I begin by considering the swimming behavior of a single bacterium. Then, by defining the average density of the bacteria at a given location using a volume fraction, I construct energy and Rayleighian functionals to describe the dissipative dynamics of the two-phase system. The rod shape of the bacteria defines a local average orientation, and torque balance is used to define the dynamics of this bacterial orientation.

### A single, swimming bacterium

*B. subtilis* is a peritrichously flagellated bacterium with a roughly cylindrical cell body of radius,  $R \sim 0.4 \mu\text{m}$ , and length,  $L \sim 4 \mu\text{m}$  (1). Each bacterium has  $\sim 10$  flagella (10), which are helical filaments of length  $L_f \sim 10 \mu\text{m}$ . The radius of a flagellum,  $R_f$ , is only 10 nm, though, so the volume occupied by the flagella can be considered to be negligible compared to the cell body. Therefore, the volume of a single bacterium is  $V_b \sim \pi R^2 L$ .

As a bacterium is an elongated object, its long axis defines an orientation. I define a unit vector,  $\mathbf{d}$ , that lies along this direction. When all the flagella rotate in the same fashion (i.e., counterclockwise), the flagella bundle together. The coordinated rotation of the flagella exerts a propulsive force on the fluid. An equal but opposite force is exerted on the bacterium

from the fluid. I assume that this thrust force lies along  $\mathbf{d}$  with magnitude  $F_0$  (Fig. 1). This force is the stall force, i.e., the force that would be required to stop a bacterium swimming in a stationary fluid.

As the Reynolds number is  $\ll 1$ , inertial terms are negligible. Therefore, in a quiescent fluid, the drag force from the fluid must balance the thrust force so that the sum of the forces on the bacterium is zero. According to slenderbody hydrodynamics, the drag force on an elongated object is proportional to the velocity difference between the fluid and the swimming bacterium. Treating both the cell body and the flagella as filamentary objects and ignoring the pitch of the flagella, the drag coefficient for motion along the long axis of the bacterium is  $\zeta_{\text{sh}} = 2\pi\eta_f L/(\ln(L/2R) + c) + 2\pi\eta_f L_f/(\ln(L_f/2R_f) + c)$  (11), where  $\eta_f$  is the fluid viscosity and  $c$  is a constant of order 1. Here the first term is the drag on the cell body and the second term is the drag on the flagella; I have treated the flagellar bundle as a single filamentary object. If an isolated bacterium swims with an average velocity  $V_0$  in a stationary fluid, then  $F_0 = \zeta_{\text{sh}} V_0$ .

Thrust force is localized at the flagella, whereas drag force is distributed over the entire bacterium. Therefore, the centers of thrust and drag are not coincident. I denote the centers of thrust and drag as  $\mathbf{x}_T$  and  $\mathbf{x}_D$ , respectively, and assume that these locations are separated by a distance  $b$  along the direction  $\mathbf{d}$ :  $\mathbf{x}_T = \mathbf{x}_D - b\mathbf{d}$  (Fig. 1).

In a fluid with an externally generated pressure gradient (i.e., a pressure gradient not generated by the swimming

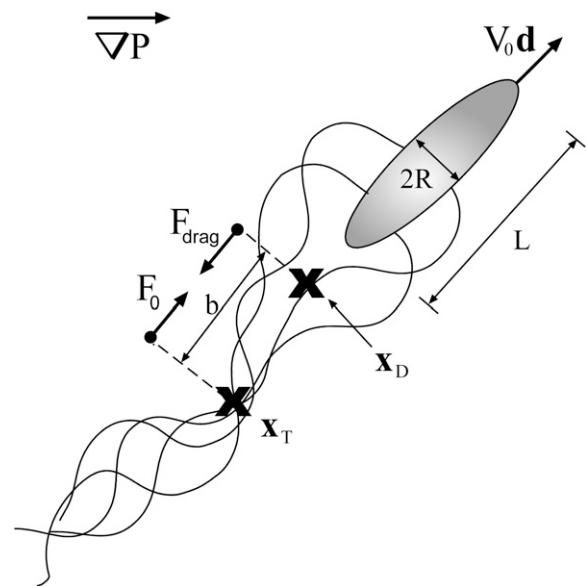


FIGURE 1 Schematic of a rod-shaped swimming bacterium in an external pressure gradient. The bacterium has length  $L$  and radius  $R$ . The bacterium exerts a force on the fluid  $\mathbf{F}_0 = 2\pi\eta_f V_0 \mathbf{d}$ , where  $\mathbf{d}$  is the direction of the long axis of the bacterium and  $V_0$  is the free swimming velocity of the bacterium. The thrust of the bacterium is produced by rotation of the flagella, and the center of thrust is defined to be at  $\mathbf{x}_T$ . The fluid exerts a drag force,  $\mathbf{F}_{\text{drag}}$ , on the bacterium. Because the bacterial body experiences drag but does not exert thrust, the center of drag,  $\mathbf{x}_D$ , is not located at  $\mathbf{x}_T$  but instead is positioned at  $\mathbf{x}_D = \mathbf{x}_T + b\mathbf{d}$ .

bacterium), the bacterium also experiences a force from the pressure field. Because the Stokes equations are linear, the pressure field can be broken into two components. One describes the pressure field generated by the motion of the bacterium, the force from which is included in the slender-body drag coefficient. The other piece is the external pressure field. In a constant external pressure gradient, the total force on the bacterium from this component of the pressure field is

$$\begin{aligned}\mathbf{F}_p &= - \int \mathbf{P} \mathbf{n} dS \\ &= -V_b \nabla P,\end{aligned}\quad (1)$$

where  $P$  is the external pressure field,  $\mathbf{n}$  is the normal vector to the surface of the bacterium, and the integral is taken over the surface of the bacterium. The divergence theorem is used to calculate the integral. Therefore, in a fluid with an external pressure gradient that varies slowly over a distance the size of a bacterium, the total force on a swimming bacterium is

$$\mathbf{F}_{\text{thrust}} + \mathbf{F}_{\text{drag}} + \mathbf{F}_p = 0. \quad (2)$$

Other forces can be added to this description to take into account Brownian motion or other random processes as well as interactions between other bacteria. However, for my purposes here, I would like to describe a dense colony of bacteria for which it will be easier to use a continuum description.

### The volume fraction

It is convenient to describe a continuum field of bacteria using the volume fraction,  $\phi_b$ , which is the fraction of space filled by bacteria in a given volume,  $V$ . The fluid volume fraction is  $\phi_f = 1 - \phi_b$ . I choose a simplified method for describing the volume fraction. Treating the center of drag of the  $i$ th bacterium,  $\mathbf{x}_{D,i}$ , as a point source for volume, the volume fraction at point  $\mathbf{x}$  can be defined as

$$\phi_b(\mathbf{x}) = \frac{1}{V} \int \sum_i V_b \delta^3(\mathbf{x} - \mathbf{x}_{D,i}) d^3X, \quad (3)$$

where  $\delta^3(\mathbf{x})$  is the three-dimensional Dirac  $\delta$ -function, and the integral is taken over a volume element,  $V$ , centered about  $\mathbf{x}$ .  $V$  is taken to be large compared to the size of a single bacterium yet small compared to the length scales over which the fluid patterns occur.

Using this definition of  $\phi_b$ , it is straightforward to calculate the average of bacterial variables inside  $V$ . For example, I define the average velocity of the bacteria at point  $\mathbf{x}$  as

$$\begin{aligned}\mathbf{v}_b(\mathbf{x}) &\equiv \left\langle \frac{d\mathbf{x}_{D,i}}{dt} \right\rangle_v = \frac{\int \sum_i \frac{d\mathbf{x}_{D,i}}{dt} \delta^3(\mathbf{x} - \mathbf{x}_{D,i}) d^3X}{\int \sum_i \delta^3(\mathbf{x} - \mathbf{x}_{D,i}) d^3X} \\ &= \frac{V_b}{V\phi_b} \int \sum_i \frac{d\mathbf{x}_{D,i}}{dt} \delta^3(\mathbf{x} - \mathbf{x}_{D,i}) d^3X.\end{aligned}\quad (4)$$

Taking the time derivative of the volume fraction (Eq. 3), I get the dynamic equation for  $\phi_b$ ,

$$\frac{d\phi_b}{dt} = -\frac{V_b}{V} \int \sum_i \nabla(\delta^3(\mathbf{x} - \mathbf{x}_{D,i})) \times \frac{d\mathbf{x}_{D,i}}{dt} d^3X. \quad (5)$$

Because the integral is over fixed limits, the gradient operator can be pulled outside the integral. Using the equation for the average bacterial velocity (4), the dynamic equation for  $\phi_b$  is a continuity equation:

$$\frac{\partial \phi_b}{\partial t} = -\nabla \cdot (\phi_b \mathbf{v}_b). \quad (6)$$

The fluid volume fraction also satisfies a continuity equation,

$$\frac{\partial \phi_f}{\partial t} = -\nabla \cdot (\phi_f \mathbf{v}_f), \quad (7)$$

where  $\mathbf{v}_f$  is the fluid velocity.

### Two-phase flow dynamics

Viscous fluid dynamics is inherently dissipative. In the low Reynolds number regime, dissipative forces (and forces that arise from energy production) are balanced by conservative forces. An elegant method for handling dissipative dynamics is to define an energy functional,  $E$ , that describes the conservative forces and a Rayleigh dissipative functional,  $R$ , to describe the dissipative forces. This technique has been used previously in the context of two-phase flows to describe polymer solutions (12). An alternative method for deriving two-phase flow equations directly averages the dynamic equations and leads to an equivalent formulation (13). The two-phase formalism has been used extensively. For example, it has been used to describe the dynamics of the eukaryotic cytoskeleton (14,15), the swelling of porous media (16), tissue deformation (17), and the nonlinear swelling of polymer gels (18).

For the collective swimming of bacteria, I define two components of the energy. The first is due to random motions of the bacteria and fluid, which leads to entropic mixing. I use the Flory-Huggins mixing energy (19),

$$E_{\text{mix}} = \frac{\zeta_{\text{sh}} D_b}{V_b} \int \phi_b \ln \phi_b d^3x + \frac{k_B T}{V_f} \int \phi_f \ln \phi_f d^3x. \quad (8)$$

Since the bacteria experience thermal fluctuations and may also execute run-and-tumble swimming, I use the fluctuation-dissipation theorem to define an energy scale,  $\zeta_{\text{sh}} D_b$ , for the bacterial mixing, where  $D_b$  is a diffusion coefficient that takes into account thermal and swimming stochasticity.  $k_B T$  is thermal energy, and  $V_f$  is the size of a water molecule. The second term in this equation is the fluid mixing entropy. For  $\phi_b \ll 1$ , a redefinition of the mechanical pressure can account for this term. As I will be considering situations when  $\phi_b < 0.2$ , I will neglect it in the rest of my calculations.

The second component of the energy comes from the constraint that in a given volume the sum of the bacterial and

fluid volume fractions must sum to 1. Defining a Lagrange multiplier,  $P$ , the constraint energy is

$$E_c = \int P(\phi_b + \phi_f - 1)d^3x \quad (9)$$

$P$  turns out to be the total mechanical pressure that maintains volume conservation. The total energy is  $E = E_{\text{mix}} + E_c$ .

There are two sources of dissipation. First, the fluid is viscous. In addition, I also allow for the possibility that bacterial collisions and interactions between the flagella may lead to an effective bacterial viscosity,  $\eta_b$ . The rod shape of the bacteria can also give rise to a number of other dissipative terms that are not considered here (see Sonnet et al. (20)). The Rayleigh dissipative functional for these viscous interactions is

$$R_{\text{vis}} = \int \left( \frac{\eta_b}{2} \mathbf{D}_b \cdot \mathbf{D}_b + \frac{\eta_f}{2} \mathbf{D}_f \cdot \mathbf{D}_f \right) d^3x, \quad (10)$$

where  $\mathbf{D}_* = (\nabla \mathbf{v}_* + (\nabla \mathbf{v}_*)^T)/2$  is a rate of strain tensor for either phase and  $* = b, f$ . Minimization of  $R_{\text{vis}}$  leads to the Newtonian viscous stress force per volume.

Viscous drag between the fluid and bacteria is the second form of dissipation. I use the fact that the drag force is proportional to the velocity difference between the bacteria and fluid and define a drag coefficient,  $\zeta$ . Therefore, the drag dissipation functional is

$$R_{\text{drag}} = \int \frac{\zeta}{2} |\mathbf{v}_b - \mathbf{v}_f|^2 d^3x. \quad (11)$$

To estimate the value for  $\zeta$ , I assume that the total drag per volume is equal to the sum of the drags on each bacterium individually; i.e., I neglect the effect of hydrodynamic interactions between the bacteria on  $\zeta$ . Therefore,  $\zeta = \phi_b \zeta_{\text{sh}}/V_b \sim 2\eta_f \phi_b (L + L_f)/R^2 L$ , where I have left off the logarithmic dependence in the denominator. This value is close to the first order approximation derived from the Darcy permeability for flow between a collection of spheres (21). For simplicity, I have chosen a scalar,  $\zeta$ , which assumes that drag on the bacteria does not depend on whether the relative velocity of the bacteria is along  $\mathbf{d}$  or perpendicular to it; however, slenderbody hydrodynamics predicts that the drag coefficient for motion perpendicular to the long axis is twice that for motions along the long axis.

The rotation of the flagella inputs energy into the system. Therefore, I also add an energy production term to the dissipative functional. The total force produced at a given position  $\mathbf{x}$  comes from all the bacteria whose center of thrust lies at point  $\mathbf{x}$ . Since it is possible for bacteria whose centers of drag are located at different locations to have the same center of thrust, the total force at a given location is a sum over all bacteria whose centers of thrust coincide with the point of interest; i.e., the total force produced at  $\mathbf{x}$  is

$$\mathbf{F}(\mathbf{x}) = \int \frac{F_0 \phi_b(\mathbf{x}') \mathbf{d}(\mathbf{x}')}{V_b} \delta^3(\mathbf{x}' - b\mathbf{d} - \mathbf{x}) d^3x'. \quad (12)$$

Here I have used the fact that the orientational vector  $\mathbf{d}(\mathbf{x})$  represents the average orientation of the bacteria in a small

volume about  $\mathbf{x}$ . Note that the force produced by the bacteria at point  $\mathbf{x}'$  acts on the bacteria located at point  $\mathbf{x}'$ ; however, the equal but opposite force acts on the fluid at point  $\mathbf{x}$ . Therefore, the energy production component of the dissipative functional is

$$R_T = - \int d^3x \int d^3x' \frac{F_0}{V_b} \phi_b(\mathbf{x}') \mathbf{d}(\mathbf{x}') \cdot (\mathbf{v}_b(\mathbf{x}') - \mathbf{v}_f(\mathbf{x})) \delta^3(\mathbf{x}' - b\mathbf{d} - \mathbf{x}). \quad (13)$$

The minus represents the fact that this term is energy production. The total Rayleigh dissipation functional is  $R = R_{\text{vis}} + R_{\text{drag}} + R_T$ .

The dynamic equations for the bacterial and fluid phases, respectively, are derived from these functionals using a variational principle:

$$\begin{aligned} \frac{d}{dt} \left( \frac{\delta E}{\delta \mathbf{v}_b} \right) - \frac{\delta E}{\delta \mathbf{x}_D} - \frac{\delta R}{\delta \mathbf{v}_b} &= 0 \\ \frac{d}{dt} \left( \frac{\delta E}{\delta \mathbf{v}_f} \right) - \frac{\delta E}{\delta \mathbf{x}_f} - \frac{\delta R}{\delta \mathbf{v}_f} &= 0. \end{aligned} \quad (14)$$

There is a minus sign difference between these formulae and the standard convention, as the energy functional has the opposite sign of the Lagrangian. It is useful to define how variations in the bacterial positions affect the volume fraction. Using a calculation similar to those in Eqs. 5 and 6, it can be shown that the variation in  $\phi_b$  is

$$\delta \phi_b = -\nabla \cdot (\phi_b \delta \mathbf{x}_D), \quad (15)$$

where  $\delta \mathbf{x}_D$  is the average variation in the bacterial position over a small volume centered about  $\mathbf{x}$ . A similar equation holds for  $\phi_f$ . Using Eqs. 14 and 15, I get the dynamic equation for the bacterial velocity,

$$\begin{aligned} &\underbrace{-\zeta(\mathbf{v}_b - \mathbf{v}_f)}_{\text{drag force}} + \underbrace{\eta_b \nabla \cdot (\nabla \mathbf{v}_b + \nabla \mathbf{v}_b^T)}_{\text{viscous stress}} + \underbrace{\frac{F_0 \phi}{V_b} \mathbf{d}}_{\text{thrust force}} \\ &\underbrace{-\frac{\zeta_{\text{sh}} D_b}{V_b} \nabla \phi}_{\text{diffusion}} - \underbrace{\phi \nabla P}_{\text{mechanical pressure}} = 0, \end{aligned} \quad (16)$$

where I have set  $\phi_b = \phi$ . This equation is the force balance equation for the bacterial phase. It states that the total force per unit volume that acts on the bacterial phase is zero when inertia is negligible. The first, third, and fifth terms here are exactly what would be predicted by considering the force per unit volume for a collection of noninteracting bacteria (see Eq. 2). The other two terms are bulk effects that take into account averaging over random forcing and approximate cell-cell interactions.

In a similar fashion, I can derive the force balance equation for the fluid phase:

$$\begin{aligned} &\underbrace{-\zeta(\mathbf{v}_f - \mathbf{v}_b)}_{\text{drag force}} + \underbrace{\eta_f \nabla \cdot (\nabla \mathbf{v}_f + \nabla \mathbf{v}_f^T)}_{\text{viscous stress}} \\ &\underbrace{- \int \frac{F_0 \phi(\mathbf{x}') \mathbf{d}(\mathbf{x}')}{V_b} \delta^3(\mathbf{x}' - b\mathbf{d} - \mathbf{x}) d^3x'}_{\text{thrust force}} - \underbrace{(1 - \phi) \nabla P}_{\text{mechanical pressure}} = 0. \end{aligned} \quad (17)$$

The thrust force is complicated by the fact that the center of drag and the center of thrust are not colocalized. To evaluate the first order effect from this, I treat  $b$  as a small parameter and expand the  $\delta$ -function in a Taylor series about the  $\mathbf{x}'$ :

$$\delta^3(\mathbf{x}' - b\mathbf{d} - \mathbf{x}) \approx \delta^3(\mathbf{x}' - \mathbf{x}) - b\mathbf{d} \cdot \nabla \delta^3(\mathbf{x}' - \mathbf{x}) \quad (18)$$

Using Eq. 18 and integrating the thrust force by parts, Eq. 17 simplifies to

$$\begin{aligned} & - \underbrace{\zeta(\mathbf{v}_f - \mathbf{v}_b)}_{\text{drag force}} + \underbrace{\eta_f \nabla \cdot (\nabla \mathbf{v}_f + \nabla \mathbf{v}_f^T)}_{\text{viscous stress}} - \underbrace{\frac{F_0 \phi}{V_b} \mathbf{d}}_{\text{thrust force}} \\ & - \nabla \cdot \left( \underbrace{\frac{bF_0 \phi}{V_b} \mathbf{d} \mathbf{d}}_{\text{dipole stress}} \right) - \underbrace{(1 - \phi) \nabla P}_{\text{hydrostatic pressure}} = 0. \end{aligned} \quad (19)$$

The first order term from the Taylor series expansion leads to a dipole stress exerted on the fluid phase from the bacterial phase (5). This dipole stress is the stress due to a pusher force, as is expected for *B. subtilis*. For puller forces, the dipole stress has the opposite sign.

The total force on the two-phase system is the sum of Eqs. 16 and 19:

$$\begin{aligned} & \eta_f \nabla \cdot (\nabla \mathbf{v}_f + (\nabla \mathbf{v}_f)^T) + \eta_b \nabla \cdot (\nabla \mathbf{v}_b + (\nabla \mathbf{v}_b)^T) \\ & - \nabla \cdot \left( \frac{bF_0 \phi}{V_b} \mathbf{d} \mathbf{d} \right) - \nabla P - \frac{\zeta_{sh} D_b}{\pi R^2 L} \nabla \phi = 0. \end{aligned} \quad (20)$$

From this force per volume, I can define the total stress on the system:

$$\begin{aligned} \sigma_{ij}^T &= \eta_f \left( \frac{\partial v_{f,i}}{\partial x_j} + \frac{\partial v_{f,j}}{\partial x_i} \right) + \eta_b \left( \frac{\partial v_{b,i}}{\partial x_j} + \frac{\partial v_{b,j}}{\partial x_i} \right) \\ & - \frac{bF_0 \phi}{V_b} d_i d_j - \left( P + \frac{\zeta_{sh} D_b \phi}{\pi R^2 L} \right) \delta_{ij}. \end{aligned} \quad (21)$$

In the absence of external forces, continuum mechanics requires that the divergence of the total stress on a system should be equal to zero, which is satisfied by this total stress using Eq. 20.

### The orientational dynamics

To close the dynamical equations, I need to describe the dynamics for the average bacterial orientation. Since the bacteria are rod shaped, at high concentrations it is expected that there will be an entropically driven tendency for the bacteria to align, much like what occurs in nematic liquid crystals (22,23). Nematic liquid crystal theory defines a critical concentration,  $\phi_{cr} \sim R/L_{eff}$ , above which this alignment will occur. Here,  $L_{eff}$  takes into account the length of the bacterium as well as any effects due to the flagella. Therefore, I expect that  $\phi_{cr}$  is  $\sim 1\%$ . The concentrations at which these turbulent flow patterns occur have been achieved only with swimming bacteria. Therefore, whether or not nonmotile bacteria at these concentrations have a tendency to align is not known.

In two dimensions, the direction  $\mathbf{d}$  can be defined by the angle  $\theta$  measured from the  $x$  direction:  $\mathbf{d} = \cos\theta \mathbf{x} + \sin\theta \mathbf{y}$ . The entropic tendency to align gives rise to an effective elasticity, such that there is an energetic cost for splay, twist, and bend variations in the direction  $\mathbf{d}$ . The magnitude of the elastic restoring force is set by the three Frank elastic constants  $K_1$  (splay),  $K_2$  (twist), and  $K_3$  (bend). In two dimensions, the twist energy is zero. I choose  $K_1 = K_3 = K$ . If the bacteria behave as rigid rods,  $K = c\epsilon\phi^2 L^2/R^3$  (24–27), where  $c$  is a constant of proportionality and  $\epsilon$  is an energy scale. For rotational diffusion driven by thermal energy,  $\epsilon = k_B T$ , with  $k_B$  being Boltzmann's constant and  $T$  the temperature. In addition, this same elasticity can give rise to additional Ericksen stresses in the fluid equation (22,28); however, I assume that these terms are negligible in comparison to the dipole stresses induced by self-propulsion, which should be true at long wavelengths in the ordered state.

If the rotational diffusion is driven by the run-and-tumble behavior of the bacteria, then the fluctuation-dissipation theorem suggests that  $\epsilon$  should be  $\sim \zeta_{sh} D_b$ . For this work, I choose the constant of proportionality to be in the range  $(0.2 - 0.4)/\pi^2$  (26). Drag due to rotations of the bacteria is balanced by the nematic, elastic torque. Rotational velocity of the fluid,  $\boldsymbol{\omega}_f = (1/2)\nabla \times \mathbf{v}_f$ , can exert torque on the bacteria. I assume a dimensionless drag coefficient for this torque,  $\zeta_r$ . For real situations, I expect that all the bacteria are not perfectly aligned along the direction  $\mathbf{d}$ . Therefore, there is a spread in the angular distribution of the bacteria. Run-and-tumble behavior of the bacteria will enhance this angular distribution. In the appendices, I show that a spread in the angular distribution leads to diffusional rotation of the bacteria. A simplified form of the full hydrodynamics of nematics (see, for example, DeGennes and Prost (22) and Yue et al. (29)) is used to define the rotation of the orientational field,  $\mathbf{d}$ :

$$\begin{aligned} \frac{\partial \mathbf{d}}{\partial t} &+ \underbrace{(\mathbf{v}_b \cdot \nabla) \mathbf{d}}_{\text{advection}} - \underbrace{\boldsymbol{\omega}_b \times \mathbf{d}}_{\text{rotation}} \\ &= \frac{1}{\zeta_r} \nabla \cdot \underbrace{(K \phi \nabla \mathbf{d})}_{\text{nematic torque}} - \zeta_f \underbrace{(\boldsymbol{\omega}_f \times \mathbf{d})}_{\text{fluid torque}} \\ &\quad - \underbrace{cV_0 \mathbf{d} \times (\mathbf{d} \times \nabla \phi + \nabla \times \mathbf{d})}_{\text{run-and-tumble diffusion}}, \end{aligned} \quad (22)$$

where  $\boldsymbol{\omega}_b = (1/2)\nabla \times \mathbf{v}_b$  and I use  $\zeta_r = \eta_f L^2 \phi / 6R^2$  for the rotational drag coefficient. In principle, the dynamics of the director can also depend on the symmetric part of the velocity gradient tensor (28). For simplicity, I ignore those terms here. In terms of  $\theta$ ,

$$\begin{aligned} \frac{\partial \theta}{\partial t} &= \frac{1}{\zeta_r} \nabla \cdot (K \nabla \theta) + \frac{1}{2} \left( \frac{\partial v_{bx}}{\partial y} - \frac{\partial v_{by}}{\partial x} \right) - \frac{\zeta_f}{2} \left( \frac{\partial v_{fx}}{\partial y} - \frac{\partial v_{fy}}{\partial x} \right) \\ &\quad - \mathbf{v}_b \cdot \nabla \theta - cV_0 \hat{\mathbf{z}} \cdot (\mathbf{d} \times \nabla \phi + \nabla \times \mathbf{d}), \end{aligned} \quad (23)$$

where  $v_{bx}$  and  $v_{by}$  are the  $x$  and  $y$  components of the bacterial velocity, respectively, and a similar definition is used for the fluid velocity.

The closed system of equations that define the two-phase collective swimming model are Eqs. 6, 7, 16, 19, and 23.

## RESULTS

### Dimensional analysis

The model Eqs. 6, 7, 16, 19, and 23 form a complex system of partial differential equations. To begin, it is useful to define characteristic scales for the problem to explore the behavior that is expected from this system. Experiments on these systems (1,3) have measured the characteristic length, time, and velocity scales. In Dombrowski et al. (1), the characteristic time,  $\tau_c$ , and length,  $L_c$ , were defined using the temporal and spatial correlations of the velocity field, respectively. These two scales correspond roughly to the persistence time and size of the vortices. In addition, the maximum velocity in the jets was used to define the characteristic velocity,  $V_c$ . It was observed that  $V_c \sim L_c/\tau_c$ , as is expected.

In the model presented here, orientation of the bacteria is maintained by the nematic elasticity, the strength of which is set by  $K$ . A parameter with dimensions of Length<sup>2</sup>/Time (i.e., a diffusion-like coefficient) can be defined as  $K/\zeta_r$ . Using this parameter, I can define a Peclet number as the dimensionless ratio of velocity to diffusion,  $Pc \sim \zeta_r V_c L_c / K$ . The size of the vortices should occur at around the length where advection begins to dominate the nematic elasticity,  $Pc > 1$ . Therefore, I expect the characteristic length to be  $L_c \sim K/\zeta_r V_c$ .

The dipole stress from the bacteria that is exerted on the fluid is primarily balanced by the fluid viscosity. Assuming that the bacterial volume fraction is  $\phi_0$  and balancing the viscous force with the dipole force,  $\zeta_r \phi_0 V_0 b / L_c \sim \eta_f V_c / L_c^2$ , or  $V_c \sim \phi_0 V_0 b L_c / R^2$ . Combining these estimates leads to the relations

$$\begin{aligned} L_c &\sim \sqrt{\frac{KR^2}{\zeta_r b \phi_0 V_0}} \\ V_c &\sim \sqrt{\frac{bK\phi_0 V_0}{\zeta_r R^2}} \\ \tau_c &\sim \frac{R^2}{b\phi_0 V_0}. \end{aligned} \quad (24)$$

These scaling relations suggest that the velocities observed in the experiment should scale like the square root of the free swimming velocity of the bacteria multiplied by the nematic elasticity constant. The characteristic lifetime of the vortices and jets should be inversely proportional to the free swimming velocity and independent of  $K$ .

### The dynamics of bacterial turbulence

I solved the model equations on a two-dimensional,  $400 \mu\text{m} \times 400 \mu\text{m}$ , periodic domain using COMSOL Multiphysics (COMSOL, Burlington, MA). Details of the numerical method

are given in the appendices. For my simulations, I used the parameter values that are given in Table 1 and varied  $V_0$ ,  $K/\zeta_r$ ,  $R$ , and  $\zeta_r$ . All simulations used an initial condition with  $\phi(\mathbf{x}, t) = 0.15$  and  $\theta(\mathbf{x}, t) = 0$  plus a small random perturbation.

When  $V_0 = 5 \mu\text{m/s}$ ,  $K/\zeta_r = 10^{-5} \text{ cm}^2/\text{s}$ ,  $R = 0.7 \mu\text{m}$ , and  $\zeta_r = 1$ , the uniform initial condition quickly (on the order of seconds) becomes unstable and develops into a velocity field filled with jets and vortices accompanied by a nonuniform volume fraction. This turbulent behavior is initiated by the volume fraction developing into a roll-like pattern (Fig. 2). Soon after this, the velocity field begins to form vortices (Fig. 2). Within a few seconds, a persistent, turbulent-looking dynamical system is observed (Fig. 3).

In agreement with the experimental measurements (1,3), the vortices and jets in this system are transient (Fig. 3) with a timescale on the order of 1 s. To make a quantitative comparison to the experiments, I calculate the temporal correlation,  $J(t) = [\langle \mathbf{v}(\mathbf{x}, s) \rangle_s - \langle \mathbf{v} \rangle_s^2] / (\langle \mathbf{v}^2 \rangle_s - \langle \mathbf{v} \rangle_s^2)$ , and the spatial correlation,  $I(|\mathbf{r}|) = [\langle \mathbf{v}(\mathbf{x} + \mathbf{r}, t) \cdot \mathbf{v}(\mathbf{x}, t) \rangle_x - \langle \mathbf{v} \rangle_x^2] / (\langle \mathbf{v}^2 \rangle_x - \langle \mathbf{v} \rangle_x^2)$ , where  $I$  is averaged over orientations of  $\mathbf{r}$ . I find correlations similar to those observed in the experiments (1) (Fig. 4). By fitting  $J(t)$  to an exponentially decaying function, I find a timescale of 0.54 s. The anticorrelation length scale from  $I(|\mathbf{r}|)$  is estimated by eye to be  $\sim 70 \mu\text{m}$ . In addition, I find velocities as large as  $100 \mu\text{m/s}$ , which is significantly larger than the free swimming velocity that I have used for this simulation.

For this simulation, I observe a volume fraction variation of  $\sim 35\%$ . The magnitude of these variations have not been measured, but density fluctuations are observed. Another feature observed in these simulations is that the velocity typically points perpendicular to the gradients of the volume fraction.

**TABLE 1** Model parameters

Symbol	Definition	Value and Units
$\eta_f$	Fluid viscosity	0.01 dynes-s/cm <sup>2</sup>
$\eta_b$	Bacterial viscosity	Unknown, assumed to be 0
$R$	Radius of bacterium	0.4–2.0 $\mu\text{m}$ (1)
$L$	Length of bacterium	4 $\mu\text{m}$ (1)
$b$	Distance between center of drag and center of thrust	4 $\mu\text{m}$ (estimated)
$\zeta$	Drag coefficient between the bacteria and the fluid	$\sim 2\eta_f b / R^2$ (see text)
$\zeta_r$	Rotational drag coefficient	$\sim \eta_f L^2 \phi / 6R^2$ (assumed)
$\zeta_f$	Dimensionless rotational drag coefficient for the torque on the bacteria from the fluid	Between 0 and 1 (assumed)
$V_0$	Free swimming velocity of a bacterium	$\sim 1\text{--}20 \mu\text{m/s}$
$F_0$	Swimming force per bacterium	$2 \pi \eta_f L V_0$ (see text)
$D_b$	Bacterial diffusion coefficient	$10^{-7} \text{ cm}^2/\text{s}$ (1,31)
$K$	Nematic elasticity	$(1.5\text{--}3)\phi^2 \text{ pN}$ (22)
$\varepsilon$	Stochastic energy scale	$\zeta_{\text{st}} D_b$ (assumed)



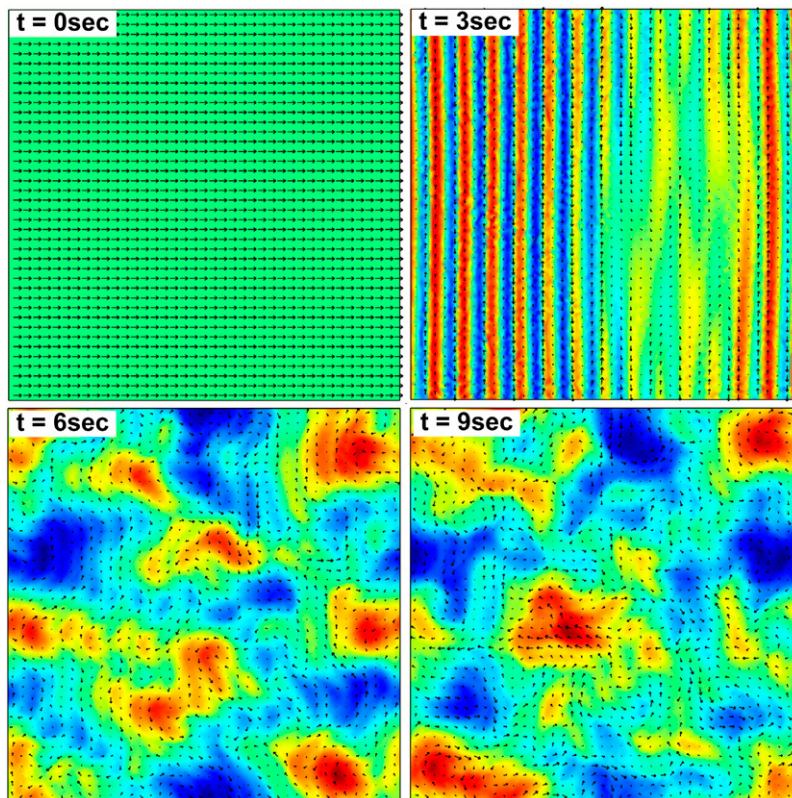


FIGURE 2 Onset of bacterial turbulence. A time series showing the bacterial volume fraction (*color map*) and the fluid velocity field (*arrows*). The simulations begin with a uniform distribution of bacteria with  $\mathbf{d}$  directed primarily along the  $x$  direction with a small random perturbation applied ( $t = 0$  s). After 3 s, the density begins to vary into a skewed roll-like pattern. After 6 s, the rolls have broken apart and vortices have formed. By 9 s, a “turbulent”-looking velocity field has emerged with high velocity jets flanked by vortices. The density fluctuations have also begun to coarsen. The range of the color map is different from frame to frame to emphasize the density variations. The parameters that were used are given in Table 1 with  $V_0 = 5 \mu\text{m/s}$ ,  $K/\zeta_r\phi = 10^{-5} \text{ cm}^2/\text{s}$ ,  $R = 0.7 \mu\text{m}$ , and  $\zeta_f = 1$ .

### Parameter dependence of the characteristic scales

To test the qualitative understanding that was presented above, a number of simulations were run that varied systematically the parameters  $V_0$ ,  $K/\zeta_r\phi$ ,  $R$ , and  $\zeta_f$ . The scaling relations (24) suggest that  $\tau_c$  should be inversely proportional to  $V_0$ , independent of  $K/\zeta_r\phi$ , and vary as  $R^2$ . In Fig. 5, *a*, *c*, and *e*,  $\tau_c$  is plotted with respect to these functions of the parameters. The scaling of  $\tau_c$  with  $V_0$  and  $R$  is seen to obey the scaling relations quite well over the biologically realistic range that was considered. From the simulations,  $\tau_c$  was found to scale with  $K^{1/2}$ , which was not accounted for in the scaling relations.

The characteristic velocity is expected to be proportional to  $V_0^{1/2}$  and to  $(K/\zeta_r\phi)^{1/2}$  and be inversely proportional to  $R$ . In Fig. 5, *b*, *d*, and *f*,  $V_c$  is plotted with respect to these functions of the parameters. For all three parameters, the scaling relations for  $V_c$  are observed to hold. At small values of  $R$ , though, I did notice some deviation from the expected scaling relations. I could not find a quantitative method for extracting the characteristic length from the spatial correlation of the fluid velocity field. However, I assume that  $L_c$  is proportional to  $V_c\tau_c$ , which is consistent with the derivation of the scaling relations.

I also ran simulations to test the effect of the fluid torque on the bacteria, the magnitude of which is determined by the parameter  $\zeta_f$ . As the bacterial force and dipole stress act along

the direction vector of the bacteria, the fluid velocity and bacterial velocity are strongly entrained to point in the same direction, even in the absence of this torque. The fluid torque acts to accentuate this orientational entrainment. Therefore, I assumed that the dynamics would not be strongly affected by the value of this parameter. Varying  $\zeta_f$  between 0 and 1 produced a relative change in  $\tau_c$  of  $\sim 40\%$  and a relative change in  $V_c$  of  $\sim 20\%$ . I also tested the dependence of the pattern formation on the magnitude of the angular spread in the orientational dynamics. I found that decreasing the value of  $c$  in Eq. 23 produced a relative increase in  $\tau_c$  of  $\sim 50\%$  and a relative decrease in  $V_c$  of  $\sim 10\%$ . Therefore, I do not expect run-and-tumble dynamics to strongly influence the pattern formation and fluid dynamics in these systems.

### DISCUSSION

In this work, I have developed a two-phase model for the swimming of dense colonies of bacteria. Using physiological parameters, the model recreates accurately the flow fields that are observed in communities of *B. subtilis*. The model is necessarily complex, taking into account swimming and alignment of the bacteria, the dipole stress that the bacteria exert on the fluid, torque from the fluid, and run-and-tumble diffusion of the bacteria. The derived and validated scaling arguments, though, shed light on the salient parameters that

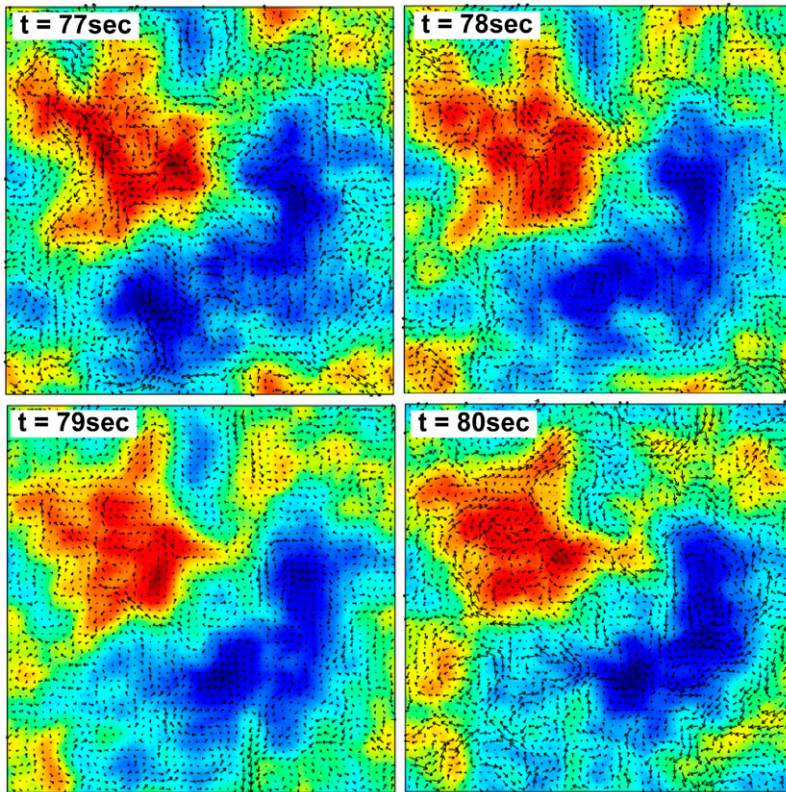


FIGURE 3 Time series showing the evolution of the fluid velocity field and bacterial density variations at times well beyond the onset of the turbulent behavior. The color map shows the bacterial volume fraction, and the arrows show the velocity field. The same parameters were used as in Fig. 2.

govern the behavior of the macroscopic flow field. In essence, the flow velocities are set by a balance between the viscosity of the fluid and the dipole stress from the bacteria, and the vortex length scale is set by a competition between advection of the bacteria and nematic alignment. The timescale for the transient nature of the flow is given by the ratio of the vortex size to the velocity.

The turbulent dynamics that are observed in this system are the long time outcome of the instability predicted in Simha and Ramaswamy (5) for suspensions of self-propelled particles with orientational order. Recent numerical studies of suspensions of discrete, self-propelled, dipole rods have also observed this instability as well as the subsequent turbulent motions (9). The model presented here advances this previous work by doing a more general derivation of the equations of motion, performing the force balance on the fluid and bacteria separately. The numerical solution of these equations shows that for physiologically realistic parameters, the model accurately describes the experimental data. In addition, the scaling arguments that are derived and validated here provide an intuitive view of the turbulent behavior in this system.

This model produces testable predictions for the dependence of the flow fields on the parameters of the system. Primary features that the characteristic scales are sensitive to are the dimensions of the individual bacteria. The length and radius of the bacterium and the length of the flagella set the drag, the nematic elasticity, and the size of the dipole stress.

Therefore, similar experiments done with different species of bacteria can provide a method for testing the validity of this model. In addition, the scaling relations suggest how the characteristic scales should depend on the average density of the bacteria. Systematically varying the density of the bacteria would also provide a test for this model.

It is interesting that the fluid flows that arise in this system are so similar to high Reynolds number flows. Specifically, the fact that von Karman street patterns with jets flanked by offset vortices are observed in flows with a Reynolds number  $> 50$  leads one to wonder what physical parameter in this low Reynolds number regime may act like a large Reynolds number. One possible solution based on this model is the effective Peclet number that was derived for the bacterial alignment,  $Pc \sim \zeta_r V_c L_c / K = \eta_f L^2 \phi_0 V_c L_c / 6 R^2 K$ . Using  $V_c = 50 \mu\text{m/s}$ ,  $L_c = 50 \mu\text{m}$ , and the parameters given in Table 1,  $Pc \sim 200$ .

Beyond the intrinsic interest in exploring an intriguing and somewhat counterintuitive biophysical phenomenon, understanding the behavior of dense colonies of bacteria has industrial and biomedical applications. The development of biofilms, which can cause infection and corrode equipment, are dependent upon the aggregation of bacteria. Also, in dead-end filtration, where water with suspended bacteria is forced through a microfilter, the bacterial concentration in the filter can reach  $10^6$ – $10^8 \text{ cm}^{-3}$  (30). How bacterial swimming affects this process has not been looked at yet.



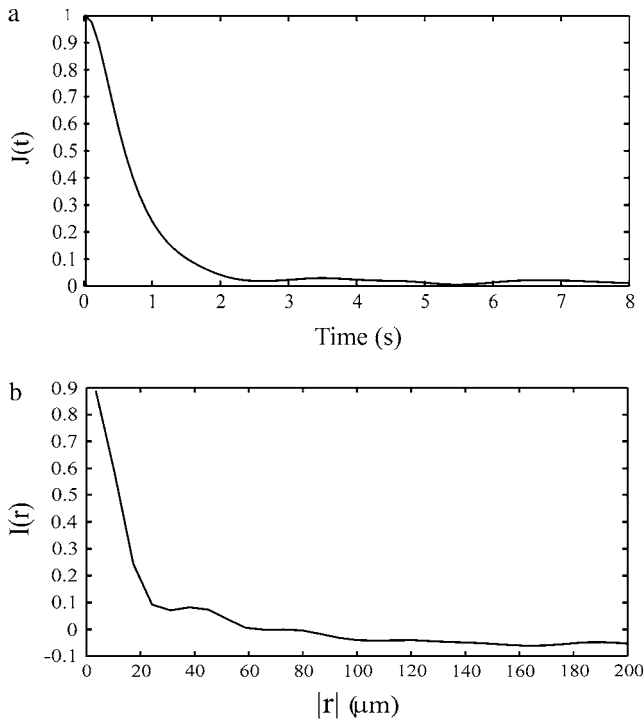


FIGURE 4 Temporal (a) and spatial (b) correlation functions of the fluid velocity field for  $V_0 = 5 \mu\text{m/s}$ ,  $K/\zeta_r = 10^{-5} \text{ cm}^2/\text{s}$ ,  $R = 0.7 \mu\text{m}$ , and  $\zeta_t = 1$ .

## APPENDIX A: CHANGES IN ANGLE DUE TO RUN-AND-TUMBLE DIFFUSION

During bacterial swimming, reversal of the flagellar motor causes the bacteria to reorient (31). These reversals happen on average every 1 s (31).

Due to these random reorientations, I expect that the bacteria in a unit volume will not all have exactly the same direction,  $\mathbf{d}$ , but rather the bacteria will have an angular distribution about this preferred direction. To analyze how run-and-tumble behavior can affect the dynamics of the preferred direction, I define the number density,  $n(\mathbf{x}, \psi, t)$ , which is the number of bacteria at point  $\mathbf{x}$  at time  $t$  aligned with angle  $\psi$  relative to the  $x$  direction. The average bacterial orientation at position  $\mathbf{x}$ ,  $\theta$ , is, therefore,

$$\theta(\mathbf{x}, t) = \frac{\int \psi n d\psi}{\int n d\psi}. \quad (\text{A1})$$

The number density of bacteria will obey the continuity equation,

$$\frac{\partial n}{\partial t} = -\nabla \cdot (n \mathbf{v}_b), \quad (\text{A2})$$

where  $\mathbf{v} = \mathbf{v}(\mathbf{x}, \psi, t)$ . Taking the time derivative of Eq. A1 and using Eq. A2, I find that

$$\frac{\partial \theta}{\partial t} = \frac{1}{N} \left( -\nabla \cdot \left( \int \psi n \mathbf{v}_b d\psi \right) + \theta \nabla \cdot \left( \int n \mathbf{v}_b d\psi \right) \right), \quad (\text{A3})$$

where I have defined the total number density of bacteria at  $\mathbf{x}$ ,  $N = \int n d\psi$ . To continue, I break the bacterial velocity into two pieces,  $\mathbf{v}_b = \mathbf{V} + \mathbf{u}$ ,  $\mathbf{V}$  is independent of  $\psi$ , and  $\mathbf{u}$  depends on  $\psi$  and is assumed to be directed along the bacterial direction,  $\mathbf{u} = u(\cos\psi \hat{\mathbf{x}} + \sin\psi \hat{\mathbf{y}})$ . Plugging this into Eq. A3 leads to

$$\frac{\partial \theta}{\partial t} = -\mathbf{V} \cdot \nabla \theta + \frac{1}{N} (\theta \nabla \cdot \int n \mathbf{u} d\psi - \nabla \cdot \int \psi n \mathbf{u} d\psi). \quad (\text{A4})$$

To make further progress in analyzing Eq. A4, I assume that  $n$  is normally distributed about  $\theta$  with a standard deviation of  $\sigma$ ,  $n = n_0 e^{-((\psi-\theta)^2)/2\sigma^2}$ . Using the identity

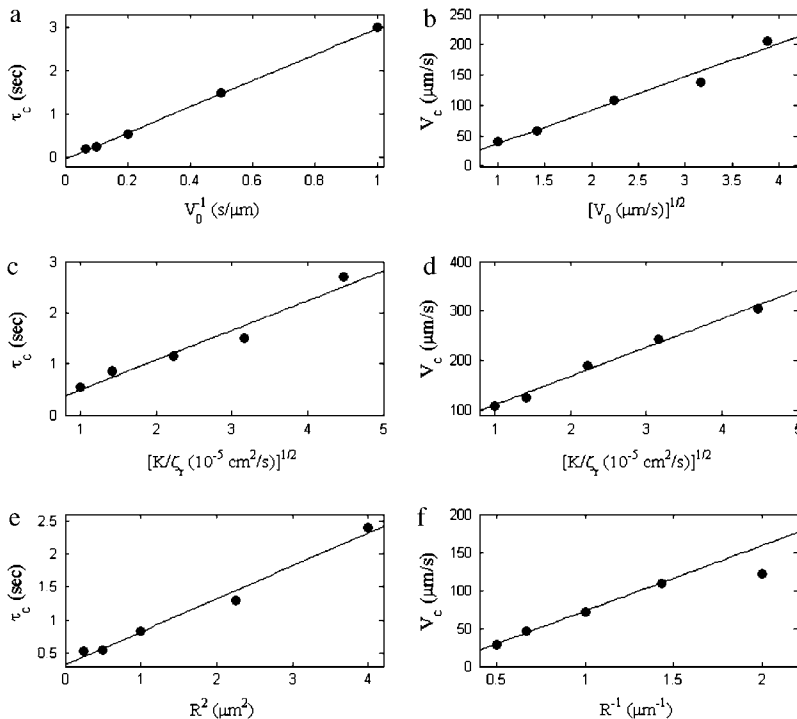


FIGURE 5 Dependence of the characteristic time and velocity on  $V_0$ ,  $K/\zeta_r \phi$ , and  $R$ . All plots are done to show the correspondence to the scaling relations given in Eq. 7. (a, c, and e)  $\tau_c$  versus  $1/V_0$ ,  $(K/\zeta_r \phi)^{1/2}$ , and  $R^2$ . (b, d, and f)  $V_c$  versus  $V_0^{1/2}$ ,  $(K/\zeta_r \phi)^{1/2}$ , and  $1/R$ . The solid lines correspond to the best fit straight line through the simulation points. All other parameters are fixed and given in Table 1.

$$\psi e^{-\frac{(\psi - \theta)^2}{2\sigma^2}} = -\sigma^2 \frac{\partial}{\partial \psi} \left( e^{-\frac{(\psi - \theta)^2}{2\sigma^2}} \right) + \theta e^{-\frac{(\psi - \theta)^2}{2\sigma^2}} \quad (\text{A5})$$

and defining the average velocity

$$\langle \mathbf{u} \rangle = \frac{1}{N} \int n \mathbf{u} d\psi, \quad (\text{A6})$$

Eq. A4 becomes

$$\frac{\partial \theta}{\partial t} = - \underbrace{(\mathbf{V} + \langle \mathbf{u} \rangle) \cdot \nabla \theta}_{\text{advection}} - \underbrace{\frac{\sigma^2}{N} \nabla \cdot n_0 \int e^{-\frac{(\psi - \theta)^2}{2\sigma^2}} \frac{\partial \mathbf{u}}{\partial \psi} d\psi}_{\text{run-and-tumble reorientation}}. \quad (\text{A7})$$

Inspection of Eq. A7 reveals that the average alignment of the bacteria is advected by the total average bacterial velocity,  $\mathbf{V} + \langle \mathbf{u} \rangle$ , and also reorients due to the spread in orientations from tumbling. To gain insight into the behavior of the reorientational term, I approximate the Gaussian function as a step function that equals 1 for  $\theta - \sigma < \psi < \theta + \sigma$  and is 0 everywhere else, and I choose  $u = V_0$ , the free swimming velocity of the bacteria. This assumption gives that  $N = 2n_0\sigma$  and the dynamic equation for  $\theta$  is

$$\begin{aligned} \frac{\partial \theta}{\partial t} &= - \underbrace{(\mathbf{V} + \langle \mathbf{u} \rangle) \cdot \nabla \theta}_{\text{advection}} - \underbrace{\frac{\sigma \sin \sigma V_0}{\phi} \nabla \cdot (\phi (-\sin \theta \hat{\mathbf{x}} + \cos \theta \hat{\mathbf{y}}))}_{\text{run-and-tumble reorientation}} \\ &= -(\mathbf{V} + \langle \mathbf{u} \rangle) \cdot \nabla \theta - \frac{cV_0}{\phi} \nabla \cdot (\phi (\hat{\mathbf{z}} \times \mathbf{d})) \\ &= -(\mathbf{V} + \langle \mathbf{u} \rangle) \cdot \nabla \theta - cV_0 \left( \hat{\mathbf{z}} \cdot \left( \mathbf{d} \times \frac{1}{\phi} \nabla \phi \right) + \hat{\mathbf{z}} \cdot \nabla \times \mathbf{d} \right), \end{aligned} \quad (\text{A8})$$

where  $c = \sigma \sin \sigma$ . For *Escherichia coli*, a single tumbling event reorients the bacterium by  $58^\circ$  (32), giving  $c = 0.86$ . In this work, I choose  $c = 1$ .

It is interesting to look at the behavior of the run-and-tumble term for the case where  $\theta = 0$  and  $\nabla \phi = \partial \phi / \partial y \hat{\mathbf{y}}$ . For this case,

$$\frac{\partial \theta}{\partial t} = -\frac{V_0}{\phi} \frac{\partial \phi}{\partial y}. \quad (\text{A9})$$

If I look at the change in  $\theta$  over a small time period,  $\tau$ ,  $\Delta \theta \approx -(V_0 \tau / \phi) (\partial \phi / \partial y)$ . Assuming that the bacterial velocity is  $\mathbf{v}_b = V_0 \mathbf{d}$  and expanding to first order in  $\Delta \theta$ , the continuity equation for the volume fraction (6) becomes

$$\begin{aligned} \frac{\partial \phi}{\partial t} &= -\nabla \cdot \left( \phi V_0 \hat{\mathbf{x}} - V_0^2 \tau \frac{\partial \phi}{\partial y} \hat{\mathbf{y}} \right) \\ &= -\nabla \cdot (\phi V_0 \hat{\mathbf{x}}) + V_0^2 \tau \frac{\partial^2 \phi}{\partial y^2}. \end{aligned} \quad (\text{A10})$$

In other words, the bacteria diffuse with diffusion coefficient  $D_b = V_0^2 \tau$ , as is traditionally assumed (31). Therefore, this term will behave similarly to diffusion.

This model is similar to one developed by Alt (33) except that here it is assumed that the angular distribution is a constant normally distributed function, whereas Alt and Brosilow et al. (34) solve for the spatial and temporal evolution of the distribution. In addition, I assume here that during tumbling, the bacteria remain at the same spatial location.

## APPENDIX B: NUMERICAL IMPLEMENTATION OF THE MODEL EQUATIONS

For all simulations, I set  $\eta_b = 0$ . This allows me to use Eq. 16 to eliminate  $\mathbf{v}_b$ ,

$$\mathbf{v}_b = \mathbf{v}_f + V_0 \mathbf{d} - \frac{D_b}{\phi} \nabla \phi - \frac{1}{\zeta} \phi \nabla P. \quad (\text{B1})$$

I also add Eqs. 6 and 7 to get a conservation equation that determines  $P$ :

$$\nabla \cdot (\phi \mathbf{v}_b + (1 - \phi) \mathbf{v}_f) = 0. \quad (\text{B2})$$

Equations B1 and B2 are used in conjuncture with Eqs. 6, 19, and 23 to solve for  $\phi$ , the two components of  $\mathbf{v}_f$ ,  $\theta$ , and  $P$ . However, I found that direct implementation of these equations into the general partial differential equation solver in COMSOL Multiphysics was unstable. I attributed this instability to the incompressibility condition (Eq. B2) and chose to use a method similar to artificial incompressibility to solve the system of equations (35). I therefore added time dependence to Eqs. 19 and B2 as

$$\begin{aligned} \varepsilon_1 \frac{\partial \mathbf{v}_f}{\partial t} &= -\zeta (\mathbf{v}_f - \mathbf{v}_b) - \zeta V_0 \mathbf{d} - (1 - \phi) \nabla P + \eta_f \nabla \\ &\quad \cdot (\nabla \mathbf{v}_f + \nabla \mathbf{v}_f^T) + \nabla \cdot (\zeta V_0 \mathbf{b} \mathbf{d} \mathbf{d}) \\ \varepsilon_2 \frac{\partial P}{\partial t} &= \nabla \cdot (\phi \mathbf{v}_b + (1 - \phi) \mathbf{v}_f), \end{aligned} \quad (\text{B3})$$

where  $\varepsilon_1$  and  $\varepsilon_2$  are small. For this scheme, I need  $\varepsilon_2$  to be less than  $\varepsilon_1$  so that the fluid velocity always feels the steady-state, incompressibility condition (Eq. B2). Chorin (35) suggests that  $\varepsilon_2 \leq \varepsilon_1/10$ . Likewise,  $\varepsilon_1 \ll 1$  guarantees that the  $\phi$  dynamics see the equilibrated fluid velocity. I found that for values of  $\varepsilon_1 < 0.01$  and  $\varepsilon_2 = \varepsilon_1/10$  the solution was well converged.

I thank R. E. Goldstein, N. G. Cogan, G. Huber, and T. R. Powers for useful discussions.

The author acknowledges support from National Science Foundation grant CTS 0623870.

## REFERENCES

1. Dombrowski, C., L. Cisneros, S. Chatkaew, J. O. Kessler, and R. E. Goldstein. 2004. Self-concentration and large-scale coherence in bacterial dynamics. *Phys. Rev. E Stat. Nonlin. Soft Matter Phys.* 93: 098103.
2. Kessler, J. O., and M. F. Wojciechowski. 1997. Collective behavior and dynamics of swimming bacteria. In *Bacteria as Multicellular Organisms*. J. A. Shapiro and M. Dworkin, editors. Oxford University Press, New York. 417.
3. Mendelson, N. H., A. Bourque, K. Wilkening, K. R. Anderson, and J. C. Watkins. 1999. Organized cell swimming motions in *Bacillus subtilis* colonies: patterns of short-lived whirls and jets. *J. Bacteriol.* 181:600–609.
4. Vogel, S. 2003. *Comparative Biomechanics*. Princeton University Press, Princeton, NJ.
5. Simha, R. A., and S. Ramaswamy. 2002. Hydrodynamic fluctuations and instabilities in ordered suspensions of self-propelled particles. *Phys. Rev. Lett.* 89:058101.
6. Voituriez, R., J. F. Joanny, and J. Prost. 2006. Generic phase diagram of active polar films. *Phys. Rev. Lett.* 96:028102.
7. Liverpool, T. B., and M. C. Marchetti. 2006. Rheology of active filament solutions. *Phys. Rev. Lett.* 97:268101.
8. Hernandez-Ortiz, J. P., C. G. Stoltz, and M. D. Graham. 2005. Transport and collective dynamics in suspensions of confined swimming particles. *Phys. Rev. Lett.* 95:204501.

9. Saintillan, D., and M. J. Shelley. 2007. Orientational order and instabilities in suspensions of self-locomoting rods. *Phys. Rev. Lett.* 99:058102.
10. Caramori, T., D. Barilla, C. Nessi, L. Sacchi, and A. Galizzi. 1996. Role of FlgM in  $\sigma^D$ -dependent gene expression in *Bacillus subtilis*. *J. Bacteriol.* 178:3113–3118.
11. Keller, J., and S. Rubinow. 1976. Slender-body theory for slow viscous flow. *J. Fluid Mech.* 44:705–714.
12. Doi, M., and A. Onuki. 1992. Dynamic coupling between stress and composition in polymer solutions and blends. *J. Phys. II.* 2:1631–1656.
13. Drew, D. A. 1983. Mathematical modeling of two-phase flow. *Annu. Rev. Fluid Mech.* 15:261–291.
14. Dembo, M., and F. Harlow. 1986. Cell motion, contractile networks, and the physics of interpenetrating reactive flow. *Biophys. J.* 50:109–121.
15. Herant, M., W. A. Marganski, and M. Dembo. 2003. The mechanics of neutrophils: synthetic modeling of three experiments. *Biophys. J.* 84:3389–3413.
16. Huyghe, J. M., and J. D. Janssen. 1997. Quadriphasic mechanics of swelling incompressible porous media. *Int. J. Eng. Sci.* 35:793–802.
17. Gu, W. Y., W. M. Lai, and V. C. Mow. 1998. A mixture theory for charged-hydrated soft tissues containing multi-electrolytes: passive transport and swelling behaviors. *J. Biomech. Eng.* 120:169–180.
18. Durning, C. J., and K. N. Morman Jr. 1993. Nonlinear swelling of polymer gels. *J. Chem. Phys.* 98:4275–4293.
19. Flory, P. 1953. Principles of Polymer Chemistry. Cornell University Press, Ithaca, NY.
20. Sonnet, A. M., P. L. Maffettone, and E. G. Virga. 2004. Continuum theory for nematic liquid crystals with tensorial order. *J. Non-Newt. Fluid Mech.* 119:51–59.
21. Happel, J., and H. Brenner. 1965. Low Reynolds Number Hydrodynamics. Prentice Hall, The Netherlands.
22. DeGennes, P. G., and J. Prost. 1995. The Physics of Liquid Crystals. Oxford University Press, Oxford, UK.
23. Onsager, L. 1949. The effects of shape on the interaction of colloidal particles. *Ann. N. Y. Acad. Sci.* 51:627–659.
24. Priest, R. G. 1973. Theory of the Frank elastic constants of nematic liquid crystals. *Phys. Rev. A.* 7:720–729.
25. Straley, J. P. 1973. Frank elastic constants of the hard-rod liquid crystal. *Phys. Rev. A.* 8:2181–2183.
26. Poniewierski, A., and J. Stecki. 1979. Statistical theory of elastic constants of nematic liquid crystals. *Mol. Phys.* 38:1931–1940.
27. Lee, S.-D., and R. B. Meyer. 1985. Computations of the phase equilibrium, elastic constants, and viscosities of a hard-rod nematic liquid crystal. *J. Chem. Phys.* 84:3443–3448.
28. Leslie, F. M. 1968. Some constitutive equations for liquid crystals. *Arch. Ration. Mech. Anal.* 28:265–283.
29. Yue, P., J. J. Feng, C. Liu, and J. Shen. 2004. A diffuse-interface method for simulating two-phase flows of complex fluids. *J. Fluid Mech.* 515:293–317.
30. Xu, W., and S. Chellam. 2005. Initial stages of bacterial fouling during dead-end microfiltration. *Environ. Sci. Technol.* 39:6470–6476.
31. Berg, H. C. 1993. Random Walks in Biology. Princeton University Press, Princeton, NJ.
32. Turner, L., W. S. Ryu, and H. C. Berg. 2000. Real-time imaging of fluorescent flagellar filaments. *J. Bacteriol.* 182:2793–2801.
33. Alt, W. 1980. Biased random walk models for chemotaxis and related diffusion approximations. *J. Math. Biol.* 9:147–177.
34. Brosilow, B. J., R. M. Ford, S. Sarman, and P. T. Cummings. 1996. Numerical solution of transport equations for bacterial chemotaxis: effect of discretization of directional motion. *SIAM J. Appl. Math.* 56:1639–1663.
35. Chorin, A. J. 1967. A numerical method for solving incompressible viscous flow problems. *J. Comput. Phys.* 2:12–26.